STEM CELLS AND DEVELOPMENT
Volume 22, Number 11, 2013

DOI: 10.1089/scd.2012.0472

Stem Cell Therapy Remediates Reconstruction of the Craniofacial Skeleton After Radiation Therapy

Sagar S. Deshpande,[1] Kathleen K. Gallagher,[1,2] Alexis Donneys,[1] Catherine N. Tchanque-Fossuo,[1] Deniz Sarhaddi,[1] Hongli Sun,[3] Paul H. Krebsbach,[3,4] and Steven R. Buchman[1]

This study utilized transplanted bone marrow stromal cells (BMSCs) as a cellular replacement therapy to remedy radiation-induced injury and restore impaired new bone formation during distraction osteogenesis (DO). BMSC therapy brought about the successful generation of new bone and significantly improved both the rate and quality of a bony union of irradiated, distracted [X-ray radiation therapy (XRT)/DO] murine mandibles to the level of nonirradiated DO animals. The bone mineral density and bone volume fraction were also significantly improved by the BMSC replacement therapy showing no difference when compared to nonirradiated animals. Finally, a biomechanical analysis examining the yield, failure load, and ultimate load also demonstrated a significantly improved structural integrity in BMSC-treated XRT/DO mandibles over XRT/DO alone. These results indicate that administration of BMSCs intraoperatively to a radiated distraction gap can function as an adequate stimulant to rescue the ability for irradiated bone to undergo DO and produce a healed regenerate of a vastly superior quality and strength. We believe that the fundamental information on the optimization of bone regeneration in the irradiated mandible provided by this work has immense potential to be translated from the bench to the bedside to lead to improved therapeutic options for patients suffering from the disastrous sequelae of radiation therapy.

Introduction

The US Surgeon General has reported that diseases of the craniofacial region are among the most common health problems affecting the general population [1]. Among these maladies, devastating head and neck cancers (HNC) single-handedly impose a significant biomedical burden by accounting for 11,400 deaths and over 50,000 new cases each year [2], with a treatment cost of nearly $2.2 trillion in the U.S. alone [3]. Historically, a number of iconic and influential figures' lives were cut short by this devastating disease. Baseball players Babe Ruth and Bill Tuttle, U.S. Presidents Grover Cleveland and Ulysses S. Grant, and entertainers George Harrison, Humphrey Bogart, and Sammy Davis Jr. were all stricken with and eventually succumbed to HNC.

Currently, most of these patients will require multimodality treatment with surgery, radiation, and chemotherapy. Although radiation has increased survival it also results in damage to adjacent normal tissues leading to significant morbidity. The corrosive impact of these radiation-induced side effects can be unrelenting and their complex management is rarely remedial. Radiation therapy changes the biologic environment of bone, resulting in a severe attenuation of cellularity and fibrosis [4,5], decreased vascular density, obliteration of small blood vessels, poor fracture and soft tissue healing [6–9], impaired growth [10], and the late devastating complication of osteoradionecrosis. The bone subjected to X-ray radiation therapy (XRT) demonstrates increased bone resorption, decreased osteogenesis, and reduced [11,12] mechanical strength [13] that predisposes the patients to the debilitating problem of late pathologic fractures with disastrous functional consequences [14]. Due to these severe problematic wound-healing issues, surgical treatment of HNC poses an ongoing challenge [15,16] and many of these patients eventually become dependent on narcotics to help alleviate their suffering. In extreme cases (like that of Roger Ebert, movie critic), radiation and failed reconstruction can lead to mandibular excision, consigning patients to suffer a life of profound pain and an inability to eat, drink, or speak.

Distraction osteogenesis (DO), the stimulation of new bone formation by the gradual separation of 2 osteogenic fronts, has become a powerful tool for reconstructing mandibular defects. The primary application of DO in Craniofacial Surgery has

[1]Craniofacial Research Laboratory, Section of Plastic Surgery, Department of Surgery, University of Michigan, Ann Arbor, Michigan.
[2]Department of Otolaryngology-Head and Neck Surgery, University of Michigan, Ann Arbor, Michigan.
[3]Department of Biologic and Materials Sciences, School of Dentistry, University of Michigan, Ann Arbor, Michigan.
[4]Department of Biomedical Engineering, University of Michigan, Ann Arbor, Michigan.

been in the setting of congenital mandibular deformities; however, the utilization of DO as a reconstructive option for tissue replacement after oncologic resection and irradiation could have immense therapeutic ramifications. This valuable reconstructive technique provides advantages over alternative methods such as Free Tissue Transfer, including avoidance of local, regional, or distant donor-site morbidity, and concurrent generation of both bone and soft tissue using a local endogenous substrate. In addition, the recovery from DO is primarily in the outpatient setting, lowering the overall cost of treatment.

Previously, we have reported on a group of experiments establishing the outcomes of a human equivalent dose of radiation in the rat mandible [17–19]. The administration of 35 Gy of radiation, fractionated over 5 days, mimics a clinical course of adjuvant radiation therapy for HNC and is a bioequivalent to 70 Gy to a human mandible. We further demonstrated that this dosage regimen would routinely lead to a pathologic nonunion in a model of murine DO that would otherwise result in normal healing [20,21].

Bone marrow stromal cells (BMSCs) are a type of adult mesenchymal stem cells that are relatively simple to harvest and culture from bone marrow tissue, and devoid of any ethical dilemmas. As the progenitor cell for osteoblasts, the BMSC can act as a cellular replacement/rejuvenation therapy for tissue damaged by radiation. Furthermore, BMSCs innately release the vascular endothelial growth factor, which, as an element of the hypoxia-inducible factor pathway (hif-1α), is responsible for inducing vasculogenesis, angiogenesis, and osteogenesis [22].

Our global hypothesis is that the pathologic effects of radiation on bone formation and healing are mediated through a mechanism of direct cellular depletion as well as diminished function of the cells responsible for the generation and maintenance of osteogenesis. The central hypothesis to be tested in this report is that the deleterious effects of radiation on bone formation can be mitigated to allow functional restoration and successful regeneration of the mandible. We posit that transplanted BMSCs provide sufficient cellular replacement and increased cell signaling to enhance the generation and quality of new bone during DO. To test this hypothesis, we utilized a novel rodent model of DO to generate specific metrics of diminished bone quality within the regenerate of irradiated, distracted mandibles, and then employed a BMSC-based tissue engineering strategy to assuage the adverse impact of a radiation-induced injury. The long-term goal of this work is to provide fundamental information that can be translated from the bench to the bedside to lead to improved treatment modalities to this severely compromised patient population.

Materials and Methods

Animal

Male Lewis Rats, ~400 g, were obtained through the University of Michigan's University Lab Animal Medicine (ULAM) department in compliance with their subdivision of the University of Michigan's Committee for the Utilization and Care of Animals (UCUCA). Rats were weighed and provided water bottles and regular chow ad libitum upon arrival to the laboratory. They were acclimated for 7 days before radiation. Animals were randomly assigned to 3 groups. (1) DO (distraction osteogenesis only, $n=9$), (2) XRT/DO (radiation therapy + distraction osteogenesis, $n=7$), (3) BMSC/XRT/DO (radiation therapy + distraction osteogenesis with intraoperative placement of 2 million BMSCs, $n=10$).

Radiation

Rat hemimandibles were irradiated using a Philips RT250 orthovoltage unit (250 kV, 15 mA) (Kimtron Medical), fractionating the dose at ~3.72 Gy/min over 5 days, for a 35 Gray total, in the Irradiation Core at the University of Michigan Cancer Center. X-Rays were utilized since they taper off quickly, affecting only the one side of the mandible, thus obviating the need for any intraoral shield. They provided the same physiologic effect on bone and soft tissue as gamma radiation does. Rats were anesthetized using Isofluorane/Oxygen (2% and 1 L/min), and then placed right side down, so only the left hemimandible was irradiated. A lead shield with a rectangular window protected the pharynx, brain, and the remainder of the animal. Dosimetry was carried out using an ionization chamber connected to an electrometer system, which is directly traceable to a National Institute of Standards and Technology calibration. This radiation protocol has been performed for several years in the department of Radiation Oncology under ULAM/UCUCA-approved protocols. The rats were maintained on regular chow and water, and observed for 2 weeks before surgery. The diet was changed to moist chow 48 h preoperatively along with Hill's high-calorie diet.

Perioperative preparation

Gentamycin [30 mg/kg subcutaneously (SQ)] was given prophylactically preop and once postop. Rats were given Buprenorphine (0.15 mg/kg SQ) along with 15 cc/kg SQ lactated ringer's solution (LR), and then anesthetized using isoflurane/oxygen throughout the surgical procedure. Animals were placed supine on a warming blanket with a protective ocular lubricant and monitored with a pulse oximeter connected to an oxygen saturation monitor.

Surgical procedure

The surgical procedure was previously described and published [23]. After standard prepping and draping with the animal on its dorsum and the neck extended, a 2-cm midline incision was placed ventrally from the anterior submentum to the neck crease. Skin flaps were elevated and secured laterally, and then the anterior-lateral mandible was exposed avoiding the mental nerve. A horizontal through-and-through defect was drilled (1/32) to pass a 1.5″ #0–80 stainless steel threaded rod across with both ends brought externally through the skin, creating the anterior portion of the modified external fixator. Then, a 1-cm incision in the midportion of the masseter muscle, directly over the inferior border of the mandible exposed the angle of the mandible, which was dissected laterally and superiorly toward the sigmoid notch and coronoid process. A small defect was drilled 2 mm anterior-superior to the mandibular angle, bilaterally, to secure a #0–80 threaded pin secured with a

titanium washer and nut, and then brought externally through the skin for the posterior fixator placement. The completed fixator was secured, and then a vertical osteotomy was created using a10-mm microreciprocating blade (Stryker) ~2 mm anterior to the posterior washer on the left hemimandible, extending from the inferior margin of the mandible superiorly to the sigmoid notch along the anterior aspect of the coronoid process. If necessary, a Surgifoam scaffold loaded with 2 million BMSCs was placed within the osteotomy (Fig. 1). The external fixator device was adjusted to insure reduction and hemostasis of the osteotomy edges. The wounds were irrigated, hemostasis verified, and then the incision was closed with staples.

Postoperative care

The animals were caged under the heat lamp and monitored with additional hydration via SQ LR, ~15 cc/kg and observed for ~1 h. Two doses of gentamycin were given Q12 h following surgery. Buprenorphine was continued (0.15–0.5 mg/kg) with 10 cc D5LR SQ Q12 h through postop day (POD)#4 and as needed thereafter, along with moist chow, a high-calorie Hill's a/d diet and water ad libitum. Bactrim was given daily to prevent infection. Pin sites were cleaned with Novalsan BID, teeth clipped weekly and staples removed by POD#14. All use and care was in compliance with UCUCA as well as the NIH *Guide for the Care and Use of Laboratory Animals* per our protocol #PRO00001267.

Distraction protocol

The distraction screw was half-turned corresponding to a 0.3 mm separation of the osteotomy fronts, beginning the pm of POD#4 and continued through the pm of POD#12. We performed a total of 17 half-turns, each on a Q12-h interval, for a total of 5.1 mm osteotomy distraction. Following DO, rats underwent 28 days of consolidation and were sacrificed on POD#40.

BMSC cultures

Bone marrow from the femoral and humeral medullary cavities was flushed with a modified Minimum Essential Medium (aMEM; Life Technologies). Cells were cultured in a growth medium [the aMEM, 2 mM glutamine, 100 U/mL penicillin, 100 μg/mL streptomycin sulfate, and 20% fetal bovine serum from preselected lots (Life Technologies)]. Cells were cultured at 37°C in an atmosphere of 100% humidity and 5% CO_2. Confluent layers of adherent cells were formed by 11–14 days. The adherent layers were harvested using the following protocol: (1) two2 washes with the Hanks' balanced salt solution (Life Technologies), (2) incubation with chondroitinase ABC (20 mU/mL; Seidaguku Corp.) in [alpha]MEM for 25–35 min at 37°C, (3) one wash with the Hanks' balanced salt solution, (4) incubation with 1× trypsin-EDTA (Life Technologies) for 25–35 min at room temperature, (5) a second incubation with trypsin-EDTA for 25–35 min at 37°C, and (6) a final wash in the growth medium. The subcultured cells were plated at 2×10^6 cells/75-cm^2 flask. Steps 2 and 3 were omitted after the second subculture of cells. Marrow cells were centrifuged at 1,000 rpm for 10 min, and the cell pellet was resuspended in a fresh [alpha]MEM containing 10% fetal bovine serum (Hyclone), 100 U/mL penicillin, and 50 μg/mL streptomycin (Life Technologies) at 37°C and 5% CO_2.

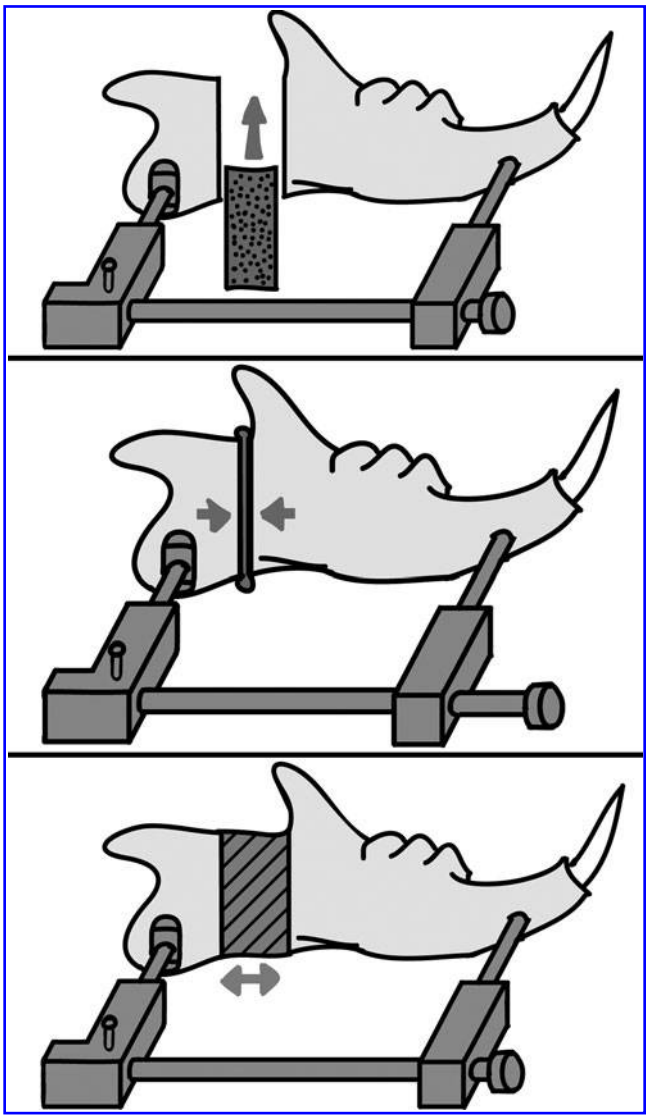

FIG. 1. Basic schematic of bone marrow stromal cell (BMSC)-assisted distraction osteogenesis (DO). *Top:* Gelatin scaffold loaded with BMSCs (*black dots*) is placed intraoperatively within the distraction gap. *Middle:* Prior to closure, the distraction gap is intraoperatively reduced and the gelatin sponge compressed so there is a boney contact between the two osseous interfaces. *Bottom:* Following a four-day latency period, an eight-day distraction period, and a 28-day consolidation period, bone is regenerated in the irradiated region of interest *(diagonal lines)*.

Loading gelatin scaffolds with cells

Each gelatin sponge was designed to be a 5×9×2-mm rectangle to match the maximum critical size defect of our distraction gap. The sponges were prewetted in the complete medium and air bubbles were removed by applying gentle pressure on the sponge between 2 pieces of sterile filter paper. Two million BMSCs were collected and suspended in 50 μL of collagen (2.5 mg/mL; rat tail collagen, type I, BD Biosciences), and loaded onto each sponge using capillary

action. Previous experiments have shown via direct cell counts (Coulter counter, model ZBI; Coulter Electronics) of the residual suspension after removal of the gelatin sponge, that when utilizing this procedure, greater than 95% of the cells entered the sponges. [24] After loading the sponges with the cells, all vehicles were incubated at 37°C for 30 min before transplantation. All procedures involving animals were performed in accordance with protocols approved by the Unit for Laboratory Animal Medicine, University of Michigan.

Transplantation of BMSCs

The gelatin sponges previously loaded with BMSCs were placed over the lateral mandible, centered within the reduced osteotomy, and medial to the dissected masseter muscle. The sponges covered the entire subperiosteal surgical mandibular region and touched the osteotomy edges throughout their inferior to superior margins.

Tissue harvest

Animals were sacrificed on postoperative day 40 via an isofluorane overdose followed by thoracotomy. Mandibles were dissected out immediately following euthanasia.

Imaging

Microcomputed tomography (Micro-CT) scan (GE Healthcare Biosciences) images were obtained using an 80 kVp, 80 mA, and 1,100 ms exposure. 392 projections were taken at a resolution of 45 microns voxel size. After initial calibration of known density standards, each complete mandible was scanned in a chilled dH_2O solution. The specimens were then immediately returned to their appropriate containers for histology or mechanical testing. The individual scans were reconstructed and reoriented in a 3-dimensional x, y, and z plane and, finally, separated into left and right hemimandibles. Each hemimandible was then reoriented with the sagittal sections following a posterior to anterior, left-to-right orientation along the x-plane. This was repeated until the sagittal, axial, and coronal sections were all aligned with a +X corresponding with the mandibular length from posterior to anterior; the +Z corresponding to the mandibular height from inferior to superior, and the +Y corresponding to the depth (or the lingual to the buccal thickness) of the mandible. Several rotations and cropping of nonbone space were undertaken to assure a uniform data analysis when the region of interest is placed corresponding with the osteotomy defects. The following specific variables will be assessed, calculated, and recorded: the bone mineral density (BMD) and bone volume fraction (BVF).

Mechanical testing—preparation of samples

Hemimandibles were split between the incisors and frozen at −20°C until testing. Just before potting, mandibles were thawed in water at room temperature. For improved adhesion of the potting medium to the specimens, small reinforcement wires were inserted perpendicularly through the hemimandibles at both the existing anterior and posterior pin-site holes. Additionally, a new hole was drilled through the condyle at the posterior superior aspect for insertion of another support wire. The 0.8-mm stainless steel reinforcement wires measured ~1.5 cm in length.

Mechanical testing—potting

Pots were cylinders machined out of aluminum, measuring 2.0 cm in diameter and 1.8 cm deep. The potting medium was a Cerrobend Bismuth Alloy (50% Bi, 27% Pb, 13% Sn, 10% Cd; MP 70°C), which when melted became an easy-to-use, conforming liquid. The posterior aspect of the mandible was potted first. The mandible was positioned inside the pot with the inferior edge of the mandible perpendicular to the top edge of the pot. The depths were determined by (and varied according to) the location of the osteotomy. Pots were placed as close to the osteotomy as possible without crossing into or over the posterior osteotomy border. Therefore, only the posterior potting depth varied between specimens, while the top edge of the pot is always perpendicular to the inferior edge of the mandible, regardless of the regenerate gap size or angle. After correct positioning was achieved, the potting medium was poured into the pot and allowed to adhere to both the pot and the specimen. Care was taken to assure that the support pins were fully buried in the medium, and that the medium is spread uniformly around the bone. To speed the adhesion, a cool air gun was utilized until the metal is hard (tested by pressing with a forceps). Pots (with ½—potted mandible) were then further cooled in an ice bath for ~60 s. The anterior portion of the mandible was potted next. Before potting, the posterior pot was precisely aligned with the new anterior pot. The anterior depth was determined anatomically by fully burying the third molar in the potting medium. Inferior edges of mandibles were again perpendicular to the top edge of the pot. After correct positioning, the potting medium was added as above and cooled similarly. Potted mandibles were stored temporarily in an ice bath until testing.

Mechanical testing—tension testing

Potted anterior–posterior hemimandibles were loaded to failure using tension at a constant displacement rate of 0.5 mm/s. We used a servohydraulic testing machine (858 Mini Bionix II; MTS Systems Corporation). A 10-lb load cell (Sensotec) was used to measure the load applied to the hemimandibles. Load head displacement was monitored with an external linear variable differential transducer (Howard A. Schaevitz Technologies, dba Macro Sensors). The load and displacement data were acquired using the TestStar IIs system (version 2.4; MTS) at a sampling frequency of 200 Hz through an A/D system (Labview; National Instruments). Load–Displacement curves were analyzed for yield and maximum load, and then, stiffness and postyield displacement were calculated and recorded.

Statistical considerations

Rats were randomly assigned to the 3 groups (DO, XRT/DO, and BMSC/XRT/DO). A 2-tailed ANOVA with the Tukey's post-test was utilized for statistical analysis, with the Levene's test for homogeneity of variances performed to ensure accurate P values. ANOVA was used as it is known to be fairly robust against small sample sizes and potentially non-Gaussian distributions. $P < 0.05$ was considered

significant. Animals were excluded from the experiment only if underwent gross infection on their left side.

Results

Gross analysis

Mandibles were first evaluated in their ability to achieve a union. The DO control group demonstrated a bony union in 8/9 animals for a rate of 89%. By contrast, XRT/DO animals resulted in a 0% union (100% nonunion). Finally, the experimental group demonstrated a bony union in 8/10 animals for a union rate of 80%. Grossly, we noticed that in XRT/DO animals, there was resorption of the posterior pin site and the angle of the mandible. Cortical thinning was also observed, exhibited by the translucency of the condyle and coronoid process. These pathologic findings were not present in the DO animals and were prevented in the BMSC/XRT/DO-treated animals (Fig. 2).

Quantitative radiomorphometry

To more specifically measure the degree by which radiation impairs new bone formation during DO and the ability of BMSCs to function as an adequate stimulant and cellular replacement therapy to remedy radiation-induced injury, rat mandibles underwent a quantitative radiomorphometric analysis via ex vivo micro-CT at a resolution of 45 μm. BVF in the XRT group demonstrated a 29% statistically significant decrease when compared to the control group. The BMSC/XRT/DO-treated animals demonstrated a 43% statistically significant increase in BVF in comparison to the XRT group. In addition the BMSC treatment was able to restore the BVF to control levels demonstrating no statistical difference between the BMSC/XRT/DO and the DO control group. The BMD analysis mirrored these same results showing a statistically significant 18.4% decrease in the XRT/DO group in comparison to the control group and a complete remediation of this mineralization metric with BMSC therapy resulting in a statistically significant 25% increase in BMD in comparison to XRT/DO (Fig. 3, Tables 1 and 2).

Biomechanical testing

Finally, biomechanical testing was performed to assess the degree by which BMSC therapy could restore structural integrity and mitigate the harmful functional impact of radiation-induced injury. Breaking strength was quantitatively assessed via tensile testing and the changes to 3 specific biomechanical properties were analyzed: the yield (Y) (the cutoff between plastic and nonplastic deformation), ultimate load (UL) (the highest load the mandible could withstand), and failure load (FL) (the final load before breaking). The Y, UL, and FL in the XRT/DO group demonstrated a massive statistically significant decrease in comparison to the control group with reductions of 97.9%, 98%, and 99.3%, respectively. The BMSC/XRT/DO-treated animals demonstrated a statistically significant increase in the Y, UL, and FL in comparison to the XRT/DO group of 1,009%, 1,679%, and 5,396%, respectively. Despite the substantial improvement that BMSC treatment was able to confer on the biomechanical properties of radiated bone, the remediation was not complete as there was still a 57.6%, 65.4%, and 66.9% respective decrease in the Y, UL, and FL when compared to the control nonirradiated animals (Tables 1 and 2).

Discussion

Mandibular DO relies on resident cellularity and vascularity to supply the site of fracture with the essential nutrition, oxygenation, growth factors, and cell populations [25]. However, radiation therapy invariably damages the areas of treatment, diminishing localized vascularity and the

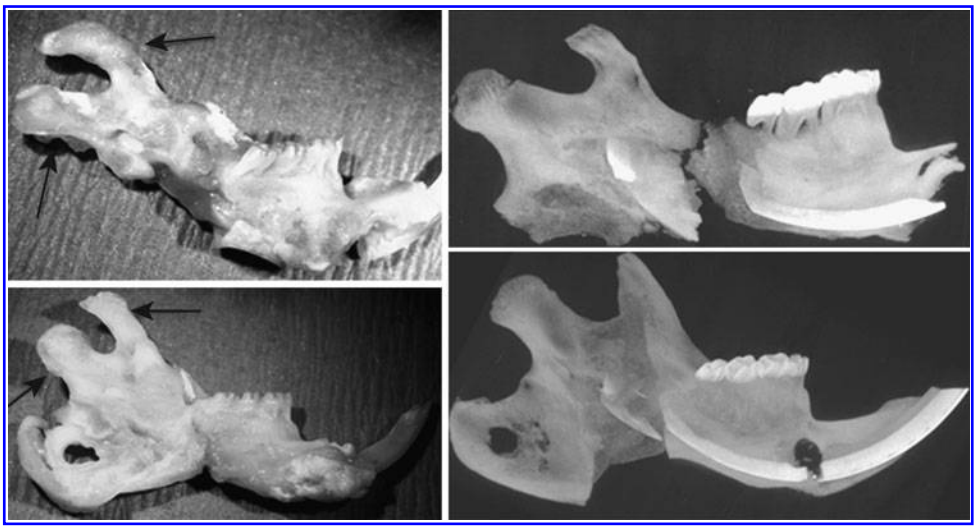

FIG. 2. Gross and Faxitron images of irradiated and BMSC-treated mandibles. *Left, top:* A photograph of an irradiated, distracted mandible. *Arrows* indicate cortical thinning. Note the fibrious union as well as the missing angle of mandible, due to resorption. *Left, bottom:* A photograph of the BMSC-treated irradiated, distracted mandible. Note the bony union as well as the robust appearance of the surrounding bone. *Right, top:* Maxmium intensity projection of the distracted, irradiated mandible. The absence of complete bony healing is readily apparent. *Right, bottom:* Maximum intensity projection of the BMSC-treated irradiated, distracted mandible. The bony regenerate spanning the distraction gap is readily apparent.

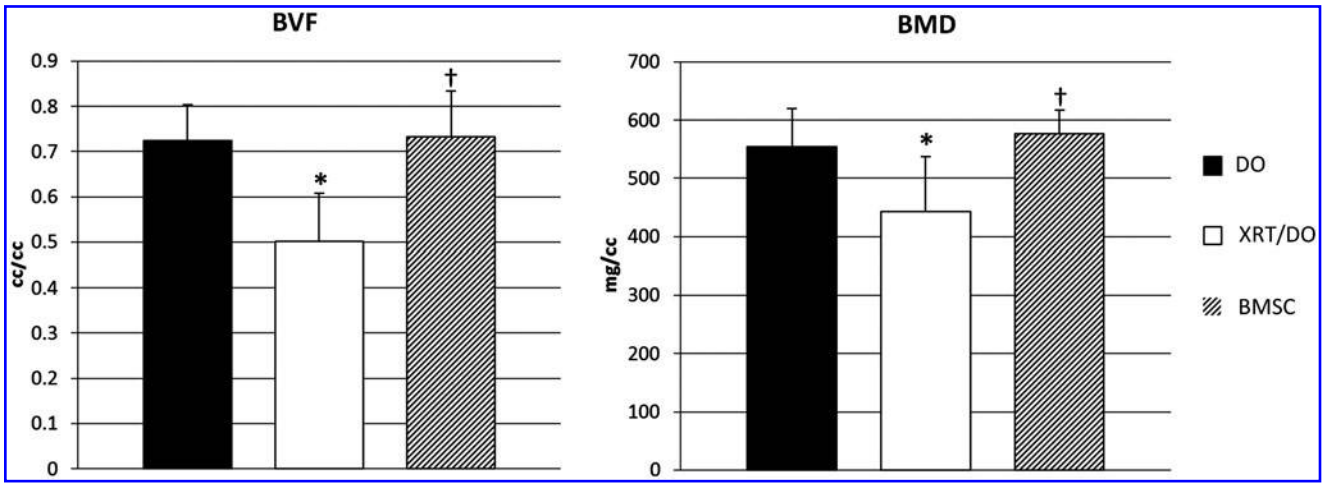

FIG. 3. Radiomorphometric parameters are remediated by BMSC-treatment to DO levels. *Left:* BMSC treatment rescued the bone volume fraction (BVF) to nonradiated levels. *Right:* BMSC treatment rescued the bone mineral density (BMD) to nonradiated levels. (*) indicates the significance between DO and X-ray radiation therapy (XRT)/DO. (†) indicates the significance between the XRT/DO and BMSC. Significance at $P \leq 0.05$.

osteocyte number, increasing the incidence of empty lacunae, and altering cytokine expression [26]. Here we report our findings that transplanted BMSC therapy provided sufficient cellular replacement to enhance the generation and quality of new bone formation during the healing process in an irradiated murine model of DO. Statistically significant improvements through the utilization of this tissue engineering strategy were demonstrated both via radiomorphometric and biomechanical response parameters, as well as overall union quality.

Exogenous BMSC therapy is an attractive candidate for craniofacial reconstruction following HNC treatment. The nature of the mandible makes it particularly susceptible to the devastating effects of radiation therapy due to its general cortical structure and lack of a large medullary cavity, which acts as a reservoir of both nutrition and stem cells. Rather, the mandible relies on a haversion-based network for nutrients and circulating stem cells for healing and reconstruction [27]. As a human-equivalent dose of radiation has devastating effects to the resident vascular network of the mandible, therapeutic doses of radiation significantly impair the ability of the bone to allow for the necessary nutrition and infiltration of progenitor cells into the wound site. As BMSCs readily incorporate into vasculogenic and osteogenic roles, exogenous administration of BMSCs overcomes the bottleneck of poor vascularity and allows for direct stimulation of the regenerate gap.

MicroCT is a powerful, rapid, and nondestructive analysis technique that allows for high-resolution 3-dimensional imagining of a given sample or region [28]. In recent years, it has become a widely utilized methodology for analyzing bone mineralization, and readily available computational technologies allow for detailed analysis of imaged regions. We demonstrated that both the BVF and BMD were returned to approximately normal, nonradiated levels utilizing a widely accepted bone threshold of 1,250 HU. The remediation of the BVF demonstrates that the percent of the regenerate that fell above this critical threshold was restored to control. The remediation of the BMD demonstrates that the overall density of the region of interest was also significantly improved, back to normal levels.

However, the ultimate gold standard of bone healing is a biomechanical response, which necessitates the use of an animal model. BMSC treatment of murine DO following radiation demonstrated a 37% remediation of the FL in comparison to control after a 28-day consolidation period. These results were vastly superior to XRT/DO, where mandibles fell apart with under a Newton of force (the force required to accelerate a 1 kg mass at 1 m/s^2). Yield (the force at which the mandible undergoes transition from plastic to

Table 1. Radiomorphometric and Biomechanical Response Parameters

	DO	*XRT/DO*	*BMSC/XRT/DO*
Bone volume fraction (unitless)	0.72 ± 0.08^a	0.51 ± 0.11	0.73 ± 0.10^a
Bone mineral density (mg/cm^3)	554.23 ± 66.29^a	452.42 ± 98.97	565.5466 ± 36.53^a
Tissue mineral density (mg/cm^3)	743.40 ± 40.07^a	670.50 ± 48.90	687.86 ± 48.02
Yield (N)	70.99 ± 21.84^a	1.49 ± 1.00	30.01 ± 5.41^a
Ultimate load (N)	93.05 ± 23.66^a	1.81 ± 0.88	32.20 ± 6.01^a
Failure load (N)	92.89 ± 23.56^a	0.56 ± 0.65	30.78 ± 6.56^a

Mean values and standard deviations for DO, XRT/DO, and BMSC/XRT/DO.
[a]Significance ($P < 0.05$) in comparison to XRT/DO.
BMSC, bone marrow stromal cell; DO, distraction osteogenesis; XRT, X-ray radiation therapy.

Table 2. *P* Values of Radiomorphometric and Biomechanical Response Data

	DO vs. XRT/DO	*BMSC/ XRT/DO vs. XRT/DO*	*DO vs. BMSC/ XRT/DO*
Bone volume fraction (unitless)	0.002	0.003	0.983
Bone mineral density (mg/cm^3)	0.044	0.048	0.962
Yield (N)	0.000	0.048	0.001
Ultimate load (N)	0.000	0.039	0.000
Failure load (N)	0.000	0.040	0.000

P values for DO, XRT/DO, and BMSC/XRT/DO.

nonplastic deformation, or the maximum force before damage occurs to the mandible) also saw comparable improvements. These results demonstrate the strategic ability of BMSCs to help remediate a pathologic, nonhealing wound.

BMSCs are currently being utilized in clinical trials for small bony defects in the craniofacial region, where they have shown to produce well-mineralized and well-vascularized jawbone regenerates [29]. Therefore, given institutional approval, there are no immediate regulatory impediments and ample precedent for the translation of this research into the operating suite. Certain precautions must be taken, however. For example, as expansion of BMSCs requires culture in fetal bovine serum, additional precautions must be taken to ensure that the cells are not exposed to the bovine spongiform encephalopathy prion. For the purposes of clinical trials, however, given that researchers abide by good tissue practice in the generation and expansion of these cells, or utilize commercial services, which isolate and purify these cells, there is no immediate impediment to the utilization of this cell population in human nonhealing defects.

Conclusion

We believe the results of this work can be built upon to further optimize the ability of bone to regenerate in the irradiated mandible as well as other areas of the appendicular skeleton by combining both cellular replacements with pharmacologic manipulation. The ability of BMSC therapy to significantly moderate the effects of radiation-induced injury and salvage impaired osteogenesis and healing during DO provides a strong evidence for the inclusion of a mesenchymal stem cell-based therapy in the treatment and reconstruction of complex skeletal injuries. We believe that the fundamental information in this report may have immense potential to be translated from the bench to the bedside to lead to improved therapeutic options for patients suffering from the disastrous sequelae of radiation therapy.

Acknowledgments

We thank the members of the Craniofacial Research Laboratory for their technical support in fulfilling this project and assisting with the significant animal care required by our model, in particular, Daniela Weiss and Noah Nelson. Furthermore, we thank the Orthopaedic Research Laboratories (headed by Dr. Steven Goldstein) and the University of Michigan Irradiation Core (headed by Dr. Mary Davis) for their assistance.

Funding: NIH-R01 CA 125187-01 (to S.R.B.).

The abstract for this data was presented at the conference of the American Society of Plastic Surgeons in 2011 and appeared in Plastic & Reconstructive Surgery for that year.

Author Disclosure Statement

The authors have no disclosures.

References

1. Allukian M. (2000). The neglected epidemic and the Surgeon General's report: a call to action for better oral health. Am J Public Health 90:843–845.
2. American Cancer Society. (2012). *American Cancer Society: Cancer Facts & Figures 2012.* American Cancer Society, Atlanta.
3. US Department of Health and Human Services. (2009). *Heathcare Cost and Utilization Project (HCUP): Outcomes by Cancer of Head and Neck.* US Department of Health and Human Services, Washington, DC.
4. Johnsson A, M Jacobsson, G Granstrom and KG Johansson. (2000). Amicroradiographic investigation of cancellous bone healing after irradiation and hyperbaric oxygenation: a rabbit study. Int J Radiat Oncol Biol Phys 48:555–563.
5. Maeda MB. (1988). Effects of irradiation on cortical bone and their time-related changes. A biomechanical and histomorphological study. J Bone Joint Surg Am 70:392–399.
6. Jacobsson M. (1985). Dynamics of irradiation injury to bone tissue. A vital microscopic investigation. ActaRadiol Oncol 24:343–350.
7. Jacobsson M, A Jonsson, T Albrektsson and I Turesson. (1985). Short- and long-term effects of irradiation on bone regeneration. Plast Reconstr Surg 76:841–850.
8. Lance A and D Markbreiter. (1989). The effect of radiation on the fracture repair process. A biomechanical evaluation of a closed fracture in a rat model. J Orthop Res 7:178–183.
9. Pelker RR, GE Friedlaender, MM Panjabi, D Kapp and ADoganis. (1984). Radiation-induced alterations of fracture healing biomechanics. J Orthop Res 2:90–96.
10. Butler MS. (1990). Skeletal sequelae of radiation therapy for malignant childhood tumors. Clin Orthop Relat Res 251: 235–240.
11. Marx RE. (1983). Osteoradionecrosis: a new concept of its pathophysiology. J Oral Maxillofac Surg 41:283–288.
12. Marx RE. (1987). Studies in the radiobiology of osteoradionecrosis and their clinical significance. Oral Surg Oral Med Oral Pathol 64:379–390.
13. Helmstedter CS, M Goebel, R Zlotecki and MT Scarborough. (2001). Pathologic fractures after surgery and radiation for soft tissue tumors. Clin Orthop Relat Res 389:165–172.
14. Aitasalo K. (1986). Bone tissue response to irradiation and treatment model of mandibular irradiation injury. An experimental and clinical study. Acta Otolaryngol Suppl 428:1–54.
15. Bengsten BP. (1993). Influence of prior radiotherapy on the development of postoperative complications and success of free tissue transfers in head and neck cancer reconstruction. Am J Surg 166:326–333.
16. Halle M. (2009). Timing of radiotherapy in head and neck free flap reconstruction—a study of postoperative complications. Plast Recon Surg 62:889–895.

17. Tchanque-Fossuo CN, LA Monson, AS Farberg, ADonneys, AJ Zehtabzadeh, ER Razolsky and SR Buchman. (2011). Dose-response effect of human equivalent radiation in the murine mandible: part I. A histomorphometric assessment. Plast Recon Surg 128:114–121.
18. Tchanque-Fossuo CN, LA Monson, AS Farberg, A Donneys, SS Deshpande, ER Razdolsky, NR Halonen, SA Goldstein and SR Buchman. (2011). Dose-response effect of human equivalent radiation in the murine mandible: part II. A biomechanical assessment. Plast Recon Surg 128:450e–487e.
19. Tchanque-Fossuo CN, A Donneys, SS Deshpande, AS Farberg, NS Nelseon MJ Boguslawski and SR Buchman. (2011). Amifostine mitigates the untoward effects of radiation on the mineralization capacity of irradiated bone in the murine mandible. Plast Recon Surg 127:83.
20. Farberg AS, XL Jing, LA Monson, A Donneys, CN Tchanque-Fossuo, SS Deshpande and SR Buchman. (2012). Deferoxamine reverses radiation induced hypovascularity during bone regeneration and repair in the murine mandible. Bone 50:1184–1187.
21. Tchanque-Fossuo CN, XL Jing, AS Farberg, ADonneys, LA Monson, SS Deshapnde and SR Buchman. (2012). Evaluation of radiation induced vascular damage in mandibular distraction osteogenesis. Plast Recon Surg 125:129.
22. Bianco P. (2001). Bone marrow stromal cells: nature, biology, and potential applications. Stem Cells 19:180–1921.
23. Buchman SR, MA IgneiziJr, C Radu, J Wilensky, AH Rosenthal, L Tong, ST Rhee and SA Goldstein. (2002). Unique rodent model of distraction osteogenesis of the mandible. Ann Plast Surg 49:511–519.
24. Krebsbach PH, MH Mankani, K Satomura, SA Kuznetsov and PG Robey. (1998). Repair of craniotomy defects using bone marrow stromal cells. Transplantation 66:1272–1278.
25. Bouletreau PJ, SM Warren and MT Longaker. (2002). The molecular biology of distraction osteogenesis. J Cranio-Maxillofac Surg 30:1–11.
26. Stone HB, CN Coleman, MS Anscher and WH McBride. (2003). Effects of radiation on normal tissue: consequences and mechanisms. Lancet Onco 4:529–536.
27. Donneys A, CN Tchanque-Fossuo, AS Farberg, XL Ling, SS Deshpande, SA Goldstein and SR Buchman. (2011). Quantitative analysis of vascular response after mandibular fracture repair utilizing micro-computed tomography with vessel perfusion. Plastic Recon Surg 127:1487–1493.
28. Kuhn JL. (1990). Evaluation of a microcomputed tomography system to study trabecular bone structure. J Orthop Res 8:833–842.
29. Kaigler D, G Pagni, CH Park, SA Tarie, RL Bartel and WV Giannobile. (2010). Angiogenic and osteogenic potential of bone repair cells. Tissue Eng Part A 16:2809–2820.

Address correspondence to:
Steven R. Buchman, MD
1540 E. Hospital Drive
4-730 C. W. Mott Children's Hospital
Ann Arbor, MI 48109

E-mail: sbuchman@med.umich.edu

Received for publication August 29, 2012
Accepted after revision December 30, 2012
Prepublished on Liebert Instant Online January 2, 2013

This article has been cited by:

1. Matthew P. Murphy, Dre Irizarry, Michael Lopez, Alessandra L. Moore, Ryan C. Ransom, Michael T. Longaker, Derek C. Wan, Charles K.F. Chan. 2017. The Role of Skeletal Stem Cells in the Reconstruction of Bone Defects. *Journal of Craniofacial Surgery* **28**:5, 1136-1141. [CrossRef]
2. Yong-Jie Wang, Jun Yan, Xiao-Li Zou, Ke-Jun Guo, Yue Zhao, Chun-Yang Meng, Fei Yin, Li Guo. 2017. Bone marrow mesenchymal stem cells repair cadmium-induced rat testis injury by inhibiting mitochondrial apoptosis. *Chemico-Biological Interactions* **271**, 39-47. [CrossRef]
3. Edward G. Carey, Sagar S. Deshpande, Kevin M. Urlaub, Alexander R. Zheutlin, Noah S. Nelson, Alexis Donneys, Stephen Y. Kang, Kathleen K. Gallagher, Peter A. Felice, Catherine N. Tchanque-Fossuo, Steven R. Buchman. 2017. Significant Differences in the Bone of an Isogenic Inbred Versus Nonisogenic Outbred Murine Mandible. *Journal of Craniofacial Surgery* **28**:4, 915-919. [CrossRef]
4. Edward G. Carey, Sagar S. Deshpande, Alexander R. Zheutlin, Noah S. Nelson, Alexis Donneys, Stephen Y. Kang, Kathleen K. Gallagher, Peter A. Felice, Catherine N. Tchanque-Fossuo, Steven R. Buchman. 2016. A Comparison of Vascularity, Bone Mineral Density Distribution, and Histomorphometrics in an Isogenic Versus an Outbred Murine Model of Mandibular Distraction Osteogenesis. *Journal of Oral and Maxillofacial Surgery* **74**:10, 2055-2065. [CrossRef]
5. Alexander R. Zheutlin, Sagar S. Deshpande, Noah S. Nelson, Stephen Y. Kang, Kathleen K. Gallagher, Yekaterina Polyatskaya, Jose J. Rodriguez, Alexis Donneys, Kavitha Ranganathan, Steven R. Buchman. 2016. Bone marrow stem cells assuage radiation-induced damage in a murine model of distraction osteogenesis: A histomorphometric evaluation. *Cytotherapy* **18**:5, 664-672. [CrossRef]
6. Yifei Du, Fei Jiang, Yi Liang, Yuli Wang, Weina Zhou, Yongchu Pan, Mingfei Xue, Yan Peng, Huan Yuan, Ning Chen, Hongbing Jiang. 2016. The angiogenic variation of skeletal site-specific human BMSCs from same alveolar cleft patients: a comparative study. *Journal of Molecular Histology* **47**:2, 153-168. [CrossRef]
7. Declan Hughes, Bing Song. 2016. Dental and Nondental Stem Cell Based Regeneration of the Craniofacial Region: A Tissue Based Approach. *Stem Cells International* **2016**, 1-20. [CrossRef]
8. Alexander R. Zheutlin, Sagar S. Deshpande, Noah S. Nelson, Yekaterina Polyatskaya, Jose J. Rodriguez, Alexis Donneys, Steven R. Buchman. 2015. A Histomorphometric Analysis of Radiation Damage in an Isogenic Murine Model of Distraction Osteogenesis. *Journal of Oral and Maxillofacial Surgery* **73**:12, 2419-2428. [CrossRef]
9. Kaitlin C. Murphy, Marissa L. Hughbanks, Bernard Y. K. Binder, Caroline B. Vissers, J. Kent Leach. 2015. Engineered Fibrin Gels for Parallel Stimulation of Mesenchymal Stem Cell Proangiogenic and Osteogenic Potential. *Annals of Biomedical Engineering* **43**:8, 2010-2021. [CrossRef]
10. B. C. Tee, Z. Sun. 2015. Mandibular distraction osteogenesis assisted by cell-based tissue engineering: a systematic review. *Orthodontics & Craniofacial Research* **18**, 39-49. [CrossRef]
11. Sagar S. Deshpande, Kathleen K. Gallagher, Alexis Donneys, Noah S. Nelson, Nicholas P. Guys, Peter A. Felice, Erin E. Page, Hongli Sun, Paul H. Krebsbach, Steven R. Buchman. 2015. Stem Cells Rejuvenate Radiation-Impaired Vasculogenesis in Murine Distraction Osteogenesis. *Plastic and Reconstructive Surgery* **135**:3, 799-806. [CrossRef]
12. Sagar S. Deshpande, Alexis Donneys, Stephen Y. Kang, Erin E. Page, Peter A. Felice, Lauren Kiryakoza, Noah S. Nelson, Jose Rodriguez, Samir S. Deshpande, Steven R. Buchman. 2014. Vascular analysis as a proxy for mechanostransduction response in an isogenic, irradiated murine model of mandibular distraction osteogenesis. *Microvascular Research* **95**, 143-148. [CrossRef]
13. Frank Boehm. Nanomedicine in Regenerative Biosystems, Human Augmentation, and Longevity 653-742. [CrossRef]
14. Sagar Deshpande, Aaron W. James, Jordan Blough, Alexis Donneys, Stewart C. Wang, Paul S. Cederna, Steven R. Buchman, Benjamin Levi. 2013. Reconciling the effects of inflammatory cytokines on mesenchymal cell osteogenic differentiation. *Journal of Surgical Research* **185**:1, 278-285. [CrossRef]